Off-The-Shelf Diodes as High-Voltage Opening Switches

Mawuena Rémi Degnon, *Student Member, IEEE*, Anton Gusev, *Member, IEEE*, Antoine Silvestre de Ferron, Laurent Pecastaing, *Senior Member, IEEE*, Gaëtan Daulhac, Aleksandr Baranov, Sébastien Boisne, and Bucur Mircea Novac, *Senior Member, IEEE*

***Abstract*—A semiconductor opening switch (SOS) (a.k.a. SOS diode) is a solid-state nanosecond switch of gigawatt power level. Due to its high pulse repetition rate, long lifetime and maintenance-free capability, the SOS diodes are becoming increasingly attractive for use in solid-state pulsed power generators. However, the lack of SOS diode manufacturers prevents the widespread use of this technology. This work demonstrates the ability of off-the-shelf diodes to operate in the SOS mode. A wide range of off-the-shelf diodes including rectifier, fast recovery, avalanche, and transient-voltage-suppression (TVS) diodes have been tested as high-voltage opening switches. An experimental arrangement based on a saturating pulse transformer was developed to test the off-the-shelf diodes in the SOS mode. The results obtained were compared to existent top of the range SOS diodes, used as reference. Two versions of the experimental setup with the initially stored energy of 25 mJ and 10 J were used. The following pulse parameters were obtained using the off-the-shelf diodes: (i) peak voltage impulse of 3 kV and rise time of 10 ns with a 110 Ω load (for the 25 mJ setup); (ii) peak voltage impulse of 80 kV and rise time of 20 ns with a 1 kΩ load (for the 10 J setup). Based on the parameters obtained, the door is opened for a future use of off-the-shelf diodes as opening switches in a wide range of solid-state based pulsed power systems.**

***Index Terms*—Pulsed power system, semiconductor opening switch, off-the-shelf diode, saturating pulse transformer.**

I. Introduction

THE switch is one of the fundamental components of all pulsed power system and can be either a closing or an opening type. The type of switch used depends on the way the energy is stored. Closing switches are used in capacitive (electric) energy storage (CES) systems, such as Marx generators, pulse forming lines, etc. Opening switches are used in circuits based on inductive (magnetic) energy storage (IES), which have a higher energy density than the CES [1]. According to [2], there are several fundamental differences between these two types of switches, that put the opening switch in a more attractive position for nanosecond pulsed power technology. An opening switch allows faster energy transfer, with the current cutting-off process increasing the output voltage, which results in a pulsed power gain.

However, while it is simpler to switch the energy stored in CES through conventional spark gap closing switches, the requirements on opening switches used in IES are usually challenging, particularly when it is required to switch-off, rapidly and repetitively, several kAs to generate hundreds of kVs or even a few MVs pulses [3]. Solid-state devices are widely used in power electronics, such as the insulated-gate bipolar transistor (IGBT), the gate turn-off thyristor (GTO) and the metal-oxide-semiconductor field-effect transistor (MOSFET). All these are potentially usable as opening switches, however they are currently limited either by a maximum current or by their switching characteristic speed [4]–[6]. With some very few exceptions, the plasma opening switch or the exploding wire is unsuitable for high pulsed repetition frequency (PRF) operation and has a limited lifetime [1], [2].

Towards the end of the 20$^{\text{th}}$ century, the semiconductor opening switch (SOS) effect was discovered in $p^+-p-n-n^+$ silicon diode structure by Rukin *et al.* [7]. The SOS effect is the nanosecond cutoff of high-density reverse currents in semiconductor diodes, for which a theoretical model was proposed in [8]. Based on this effect, SOS diodes were developed over three decades ago [9]. That sparked a breakthrough in the development of solid-state pulsed power systems based on inductive energy storage, since it allows the improvement of their important characteristics such as current density, pulsed power, voltage, energy and PRF [10], [11]. Due to high PRF of operation, long lifetime, and high average power, the SOS generators are currently used not only in research but also in modern biological, medical and industrial applications, such as X-ray pulsed sources, particle accelerators, non-thermal-plasma purification of water and gas, e-beam sterilization, laser pumping sources and many other [12]–[18].

However, the interest in the benefits of SOS for improving the performance of pulsed power systems sharply contrasts with a lack of SOS diode manufacturers. Hence, demonstrating the possibility of using off-the-shelf diodes as SOS diodes represents the main aim of the research presented in this paper. A wide range of off-the-shelf diodes have been tested as high-voltage opening switches at switching energies of up to 10 J. The results are presented in the second and third sections, respectively devoted to the 25 mJ and 10 J experimental

This research was carried out within the framework of the E2S UPPA project (S2P2 and PULPA Chairs) supported by the French "Investissements d'Avenir" programme managed by ANR (ANR-16-IDEX-0002). This work is also funded by ITHPP.

M. R. Degnon is with the Universite de Pau et des Pays de l'Adour, E2S UPPA, SIAME, Pau, France, and also with ITHPP ALCEN, Thégra, France (e-mail: rdegnon@ithpp-alcen.fr).

A. Gusev, A. Silvestre de Ferron, and L. Pecastaing are with the Universite de Pau et des Pays de l'Adour, E2S UPPA, SIAME, Pau, France (e-mail: anton.gusev@univ-pau.fr).

G. Daulhac, A. Baranov, and S. Boisne are with ITHPP ALCEN, Thégra, France (e-mail: Sboisne@ithpp-alcen.fr).

B. M. Novac is with the Wolfson School of Mechanical, Electrical and Manufacturing Engineering, Loughborough University, Loughborough, United Kingdom, and also with the Universite de Pau et des Pays de l'Adour, E2S UPPA, SIAME, Pau, France (e-mail: b.m.novac@lboro.ac.uk).

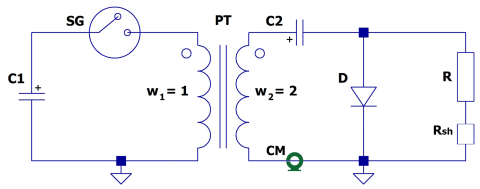

Fig. 1. Circuit diagram of the 25 mJ experimental arrangement. Explanations are provided in the text.

arrangements. The last section is devoted to conclusions.

II. The 25 mJ Experimental Arrangement

A. Circuit Description

A simplified circuit of the low-energy test bench is shown in Fig. 1. The circuit is designed with a single magnetic element to ensure high energy efficiency, which can be up to 70% [19]. For convenience, a self-breakdown spark gap SG is used as a primary switch. The ceramic capacitors C1 and C2 have a capacitance of 50 nF and 12.5 nF, respectively. The magnetic core of the pulse transformer (PT) consists of a single nanocrystalline ring (110 × 80 × 20 mm) obtained from Vacuumschmelze, with the saturation induction being 1.2 T [20]. The saturating magnetic core PT ensures two main functions. The first is to transfer the energy from the primary to the secondary circuit, stepping up the voltage. The second is to have a very low inductance of the secondary winding, when the magnetic core is driven to saturation. The primary and secondary windings of the PT have $w_1 = 1$ and $w_2 = 2$ turns, respectively. A bias winding of 2 turns (not shown) with a maximum current amplitude of 3 A is used to reset the core before the next pulse. The low-inductance resistive load R is connected in parallel to the diode D under test.

The circuit of Fig. 1 operates as follows. Firstly, C1 is charged to its initial voltage V_{C1} by an external DC power supply (not shown). When SG closes, C1 releases its energy and the PT charges C2, while the current flows through the diode D in the forward direction. For an SOS diode, this is the forward pumping stage, which lasts for t^+ while the current reaches its maximum amplitude I^+ (Fig. 2(a)). The circuit is designed using the voltage-time product [21] to reach the maximum voltage across C2 at the moment when the magnetic core of the PT saturates. At this moment, C2 starts to discharge through the secondary winding w_2 of the saturated PT, generating the reverse current through the diode. This represents the reverse pumping stage for the SOS diode, where the current reaches the maximum amplitude I^- after a duration t^- (Fig. 2(a)). The magnitude of the reverse current, and thus the reverse current density, is greater than the forward current due to the much lower self-inductance of the saturated PT. Finally, this reverse current is cut off within the switching time t_0 (Fig.2(a)) by the SOS diode and the energy is transferred to the load R, generating a very short nanosecond high-voltage pulse with a characteristic rise time Tr (Fig. 2(b)).

A reverse current with a density of more than 1 kA/cm² leads to a high electric field region, which is formed in the p region of the SOS diode structure ($p^+ - p - n - n^+$) due to the electron-hole plasma motion. Hence, in the SOS diode, the current interruption occurs in the p region rather than in the p-n junction. Details of the SOS diode physics are described in [2].

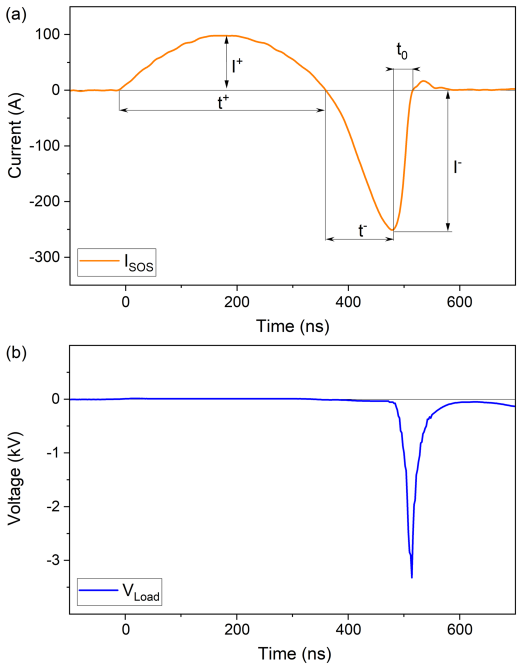

Fig. 2. Typical waveforms of the current flowing through the SOS-R diode (a), and the voltage across the load R = 28 Ω for V_{C1} = 1 kV (b).

All rise times in the present paper are defined as the time interval from 10% to 90% of the peak impulse. The charging voltage of C1 is measured using the Tektronix probe P6015A. The voltage across the load and the current through the diodes are obtained using the current measurements of the Pearson current monitor (CM in Fig. 1) model 410 and the resistive shunt Rsh = 0.9 Ω (Fig. 1). The waveforms are captured using Rigol DS1204B real-time oscilloscope.

B. Low-Voltage Diodes

25 types of off-the-shelf diodes were selected and tested as opening switches including rectifying, avalanche, Schottky, transient-voltage-suppression (TVS), and Zener diodes. The specifications of the studied diodes are as follows: blocking voltage ranging from 0.2 kV to 10 kV, die area from 0.01 cm² to 0.81 cm² and a recovery time from 0.1 µs to 20 µs. The die area of each diode was measured to calculate the cutting current density which, according to [7], must be more than 1 kA/cm² in the SOS mode of operation. SOS diodes manufactured in Russia and kindly provided by the Institute of Electrophysics having 0.25 cm² die area and 3 kV rated voltage, and here termed SOS-R, are used as a reference to which the characteristics of all the off-the-shelf units are compared to.

C. Results and Discussion

Firstly, the reference SOS-R diode is tested in the circuit shown in Fig. 1 with the charging voltage V_{C1} fixed at 1 kV.

The results obtained using the SOS-R with a load resistance R = 28 Ω are presented in Fig. 2. A forward pumping current I^+ = 100 A flows through the single SOS diode within t^+ = 380 ns. After saturation of the magnetic core of the PT, a reverse current I^- = 260 A flows through the diode for a duration t^- = 120 ns. After that, the current is cut off by the SOS-R diode within a time t_0 = 34 ns. A voltage pulse with an amplitude of 3.4 kV and a rise time of 20 ns is obtained at the load. The voltage amplitude V_{C2} measured at the capacitor C2 is 1.7 kV, which gives an SOS-R overvoltage coefficient of 2, which is defined as $K_{ov} = V_R/V_{C2}$.

Secondly, after testing the SOS-R, all the 25 selected off-the-shelf diodes were tested one by one, in the same configuration as the SOS-R diode. Fig. 3 shows all the current and voltage waveforms obtained during these tests in comparison with the results obtained from the SOS-R diode.

As a general observation, it is clear that not all diodes can operate in the SOS mode. Rectifier, avalanche, Zener and TVS diodes are able to open and transfer the current to the load. However, the switching time greatly varies. At the same time, the Schottky diodes, due to their structure and physics of operation, are not capable of reaching and interrupting the high reverse current. Small-area high-voltage diodes demonstrate a voltage drop during the forward current, which leads to additional energy losses and reduces the efficiency of the switch. Also, for most of the tested off-the-shelf diodes, the output voltage was limited to the level of the rated voltage for a switch consisting of a single diode.

To overcome the voltage limitation and to reduce the voltage drop during the forward current, a series-parallel connection of the diodes has been also studied. The parallel connection aims at reducing the voltage drop, while the series connection increases the blocking voltage capability. The even distribution of the voltage across the series connected SOS diodes [22] makes it possible to assemble the diodes without any voltage distribution circuit consideration. The best results obtained from the different types of single diodes are shown in Fig. 4(a); the improvement of the series-parallel connections can be seen in Fig. 4(b). The voltage capability of the off-the-shelf diodes is thus improved and, as a result, nanosecond voltages ranging from 1.8 kV to 2.5 kV were obtained on the resistive load of 28 Ω instead of 0.5 kV to 1.4 kV for the single diodes. However, the highest corresponding overvoltage coefficient of the off-the-shelf diodes is 1.5, which is less than the coefficient obtained for the reference SOS-R diode that equals 2.

Even though the off-the-shelf diodes produce pulses with a voltage amplitude of about 25% less than the SOS diode, the obtained results confirm the possibility of using the off-the-shelf diodes as opening switches for IES circuits at the low energy level of 25 mJ. From a summary of the relevant parameters presented in Table I, one can see the TVS diodes, in particular, have the fastest switching time of 13 ns compared to the other types of tested diodes. In addition, the full width at half maximum (FWHM) of the off-the-shelf diodes voltages are 1.6 to 3 times longer than the SOS-R.

Furthermore, a 3.15 kV output voltage with a rise time of 10 ns and a FWHM of 40 ns was obtained on a 110 Ω load by using an assembly of 64 (8 series x 8 parallel) TVS diodes

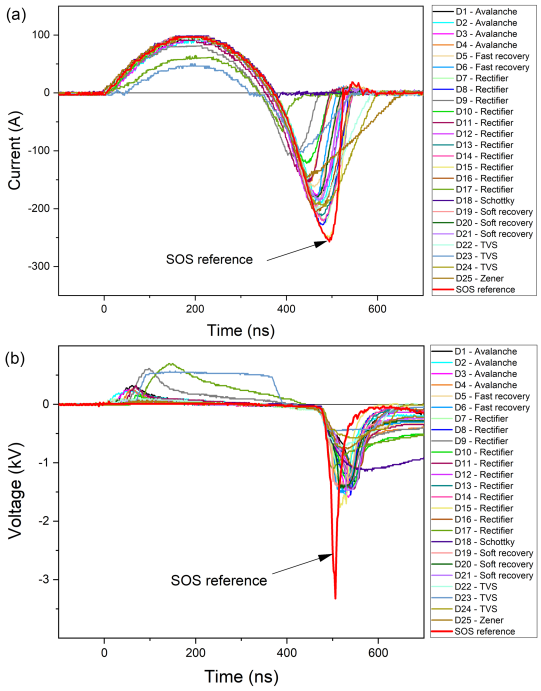

Fig. 3. Current (a) and voltage (b) waveforms of the tested off-the-shelf diodes in comparison with the SOS reference diode.

at a charging voltage across C1 of V_{C1} = 1.9 kV (Fig. 5). In this configuration, the forward current of duration t^+ = 360 ns reached an amplitude I^+ of 170 A while the reverse current after flowing for t^- = 100 ns reached the amplitude I^- of 375 A with the diode having a current cutoff time of 30 ns.

TABLE I
VOLTAGE PULSE PARAMETERS OF
THE BEST TESTED OFF-THE-SHELF OPENING SWITCHES AT :
V_{C1} = 1 KV AND R = 28 Ω

Diode type	Connections		V_R	T_r (ns)	FWHM
	Series	Parallel	(kV)	(10-90%)	(ns)
Rectifier	2	2	1.85	21.2	40
Avalanche	2	20	1.96	22.4	38
Fast recovery	2	1	2.54	27.1	28
TVS	7	3	1.83	13.2	45
SOS (Ref.)	1	1	3.35	19.5	16

III. The High Energy 10 J Experimental Arrangement

A. Circuit Description

The equivalent electrical circuit of the high-energy test bench is presented in Fig. 6. This circuit is similar to the one presented in Fig. 1. A modification of the components was however implemented in order to increase the initially stored energy and, thereby, voltage amplitude across the load. Here, the pulse transformer PT is based on a nanocrystalline magnetic core obtained from Finemet FT-3L, with the magnetic core parameters provided in [23]. The primary winding circuit consists of a film capacitor C1 = 200 nF, a triggered

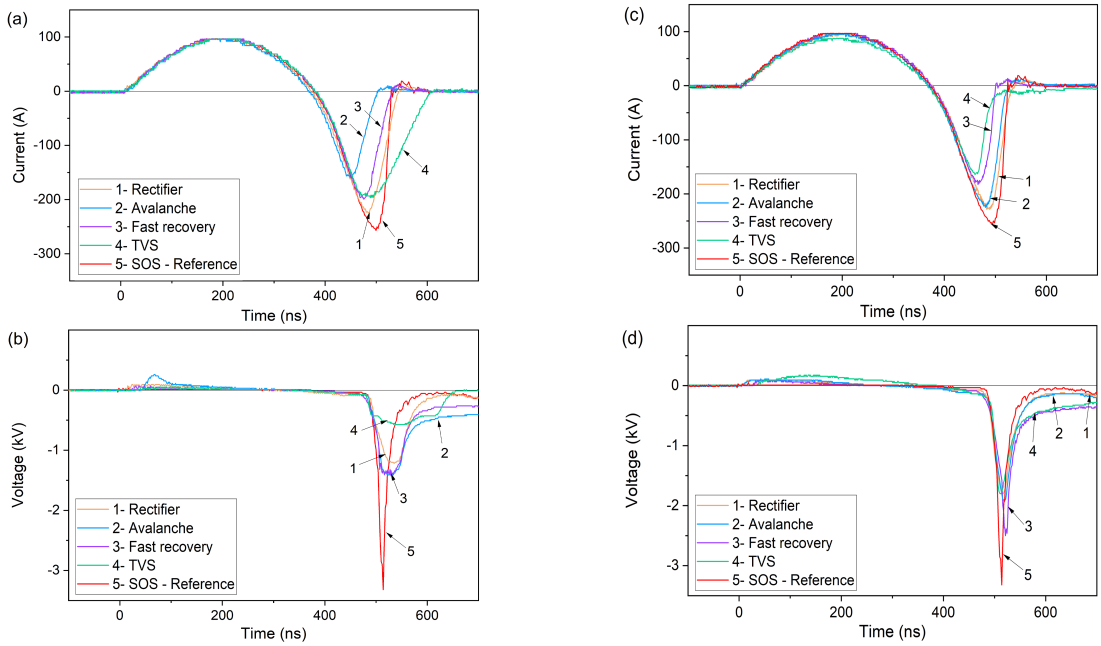

Fig. 4. The current and voltage curves of the best pulse of each type of: the single diode (a)-(b); the diodes connected in series-parallel (c)-(d) (1 - Rectifier: 2 series x 2 parallels; 2 - Avalanche: 2 series x 20 parallels; 3 - Fast recovery: 2 series; 4 - TVS: 7 series x 3 parallels) at the load of 28 Ω.

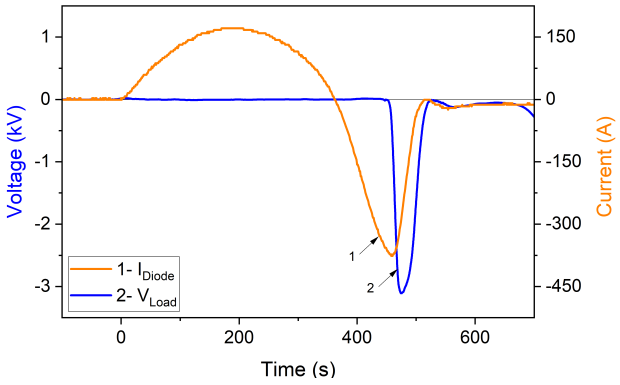

Fig. 5. Waveforms of the current flowing through the 64 (8 series x 8 parallel) TVS diodes assembly (1), and voltage pulse across the 110 Ω load at V_{C1} = 1.9 kV (2).

spark gap switch SG, and a single turn primary winding w_1. The secondary winding circuit consists of a ceramic capacitor C2 = 2 nF, a 10-turn secondary winding w_2, a diode D and a resistive load R. To prevent any breakdown, the diode and the load are both mounted under oil. Since the charging voltage of the primary capacitor is limited to 10 kV, the maximum initial electrostatic energy that can be stored is 10 J. The additional inductors L1 and L2 are further installed in order to vary the parameters of the forward and reverse pumping. The resetting circuit (not shown) consists of a 5-turn bias winding driven by a DC current source with an amplitude up to 3 A. A choke (not shown) decouples the resetting circuit from the main circuit, preventing energy losses and protecting the current source. The operation of the circuit is similar to the one previously described in Section II.

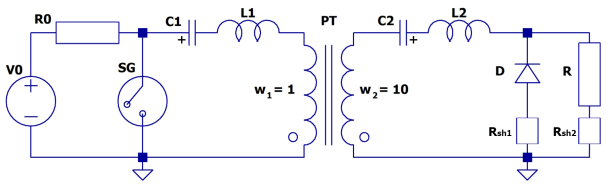

Fig. 6. Circuit diagram of the 10 J experimental arrangement. Explanations are provided in the text.

The voltages V_{C1} and V_{C2} are measured using Tektronix P6015A and Northstar PVM100 probes, respectively. The waveforms are recorded by a DS1204B Rigol oscilloscope. The currents through the diode and the load are measured by two homemade resistive shunts (0.5 Ω and 0.15 Ω) with a usable rise time of about 0.5 ns. The voltage across the load is found using Ohm's law. A 7 GHz Tektronix TDS7704B oscilloscope is used to capture the extremely fast signals generated by the diode and the load circuits. Wide bandwidth attenuators by Barth (26 dB, 30 GHz) and RF-Lambda (6 dB and 20 dB, 4 GHz) are used to attenuate the high-voltage signals obtained from the resistive shunts.

B. High-Voltage Diodes

Several elementary off-the-shelf rectifier diodes were connected in series to build a high-voltage diode assembly having an overall blocking voltage of about 100 kV. This diode is termed OTS-100. The characteristics obtained for the OTS-100 on the 10 J test bench are compared with those of the SOS-180-4 diode [19], rated for 180 kV which serves as a reference.

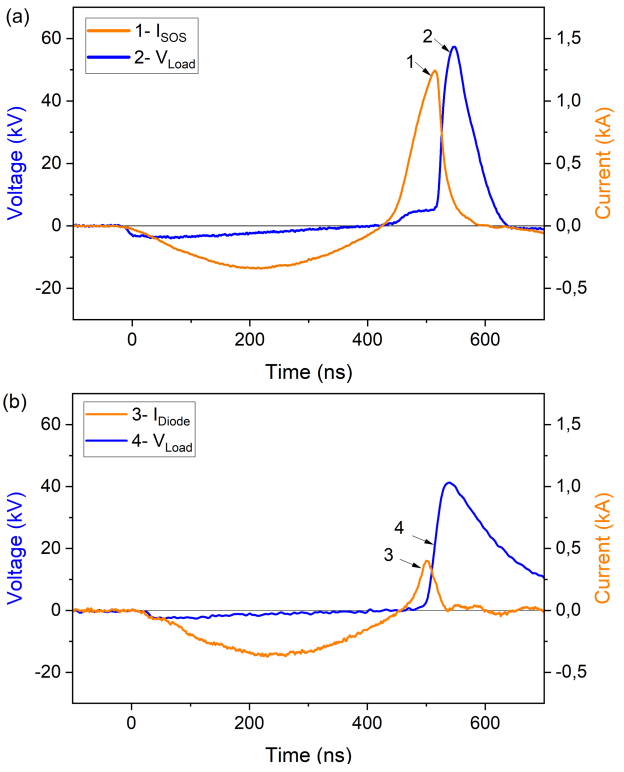

Fig. 7. Waveforms of the current through the diode D (1, 3) and voltage across the load R = 70 Ω (2, 4) at V_{C1} = 6 kV for the SOS-180-4 (a) and OTS-100 (b).

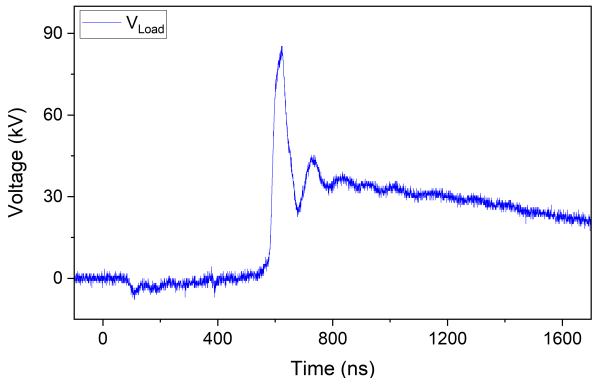

Fig. 8. Waveform of the voltage across the load R = 1 kΩ at V_{C1} = 6 kV.

C. Results and Discussion

Firstly, the SOS-180-4 diode was tested on the 10 J test bench. The charging voltage of C1 (Fig. 6) was fixed at 6 kV. A tubular non-inductive ceramic resistor R = 70 Ω was used as a load. For the SOS-180-4 diode, the following parameters were obtained (Fig. 7(a)): forward pumping current I^+ = 400 A, duration t^+ = 440 ns, reverse pumping current I^- = 1.3 kA and reverse pumping time t^- = 90 ns while the cutoff time t_0 is 32 ns. The voltage pulse generated on the resistive load has an amplitude of 58 kV with a rise time of 19 ns, and a pulse duration of 55 ns (FWHM). The overvoltage coefficient K_{ov} of the SOS-180-4 diode is 1.2.

Secondly, the current and voltage pulse parameters obtained using the OTS-100 operated under the same condition as the SOS-180-4 are as follows (Fig. 7(b)): forward pumping current I^+ = 370 A, duration t^+ = 440 ns, reverse pumping current I^- = 0.4 kA and reverse pumping time t^- = 45 ns. Cutoff time t_0 was 23 ns. The load voltage pulse has an amplitude of 42 kV, rise time of 22 ns and pulse duration of 108 ns (FWHM). The overvoltage coefficient of the OTS-100 is K_{ov} = 0.85.

Both the SOS-180-4 and OTS-100 have practically the same forward pumping parameters I^+, t^+ and voltage drop (Fig.7). However, the behavior of the OTS-100 during the reverse pumping is changing dramatically: its reverse pumping time t^- is two times less when compared to the SOS-180-4 diode. Eventually, this leads to the threefold decrease of the reverse current I^-, which prevents storing energy in the inductive energy storage (L2 and parasitic inductance). While the reverse to forward current ratio (I^-/I^+) of the SOS-180-4 is 3.2, this ratio is only 1.1 for the OTS-100. Hence, in the latter case, one part of the energy still remains stored in the C2 at the current cutoff phase. Then both parts of the energy are switched into the load. As a consequence, the voltage pulse across the load has two clearly distinguished stages (Fig. 8). The first high-voltage stage could be driven by the energy stored in the inductance L2; the second low-voltage stage could be driven by the discharge of the remaining energy in C2. Since the time constant of the capacitor discharge is increasing, this effect is accentuated for high-impedance loads. For example, for a 1 kΩ load, the complete discharge of the capacitor into the load occurs after a few μs (Fig. 8).

D. Optimization of the OTS-100 Operating Mode

This section is dedicated to an examination of the main factors affecting the reverse pumping parameters of the OTS-100 when operating as an opening switch. An experimental study was undertaken to find ways to increase the reverse pumping time, the inductive stored energy and therefore, all the output pulse parameters.

Firstly, amplitude and duration of the forward and reverse pumping currents were varied, by changing V_{C1} (Fig. 6) from 3 kV to 10 kV. During these tests, by changing V_{C1} and simultaneously adjusting the bias current, the voltage V_R across the 70 Ω load was adjusted almost linearly from 10 kV to 70 kV (Fig. 9(a)). This demonstrates a possibility of building an adjustable pulse power generator based on an opening switch combined with a saturating pulse transformer.

The maximum output voltage V_R = 70 kV with a rise time of 23 ns and duration of 100 ns (FWHM) was obtained for a 70 Ω load and for a charging voltage V_{C1} = 10 kV, which corresponds to 10 J energy stored in C1 (Fig. 9(a)). The corresponding forward and reverse currents through the OTS-100 diode are I^+ = 0.6 kA and I^- = 0.8 kA. The load current reaches 1 kA, resulting in a load peak power of 70 MW.

The influence of V_{C1} on the diode pumping is presented in Fig. 9(b) and Fig. 9(c). When V_{C1} increases, both I^+ and I^- increase, respectively, from 160 A to 650 A, and from 70 A to 800 A. At the same time, t^+ slightly decreases from 480 ns to 400 ns while t^- decreases from 80 ns to 30 ns. Consequently, the ratio of the forward to reverse current duration t^+/t^- also increases. In addition, the ratio I^-/I^+ increases from 0.4 to

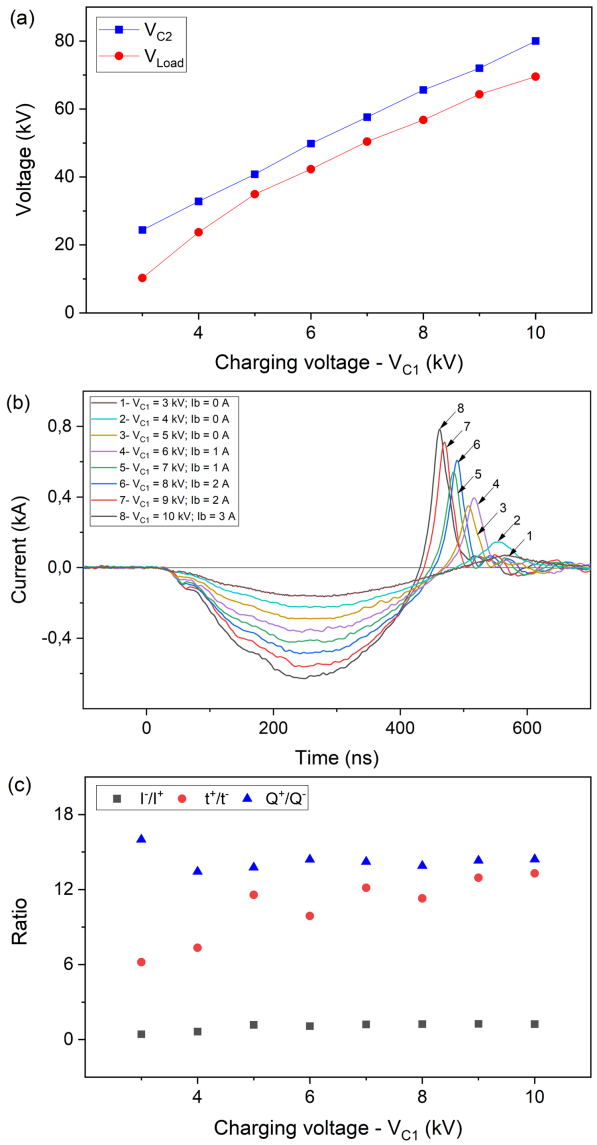

Fig. 9. Evolution of the voltages across C2 (square) and load (round) (a); current through the diode (b); ratios of the pumping currents (square), pumping times (round), and electric charges (triangle) (c) as a function of the charging voltage V_{C1} and time, using the OTS-100 diode and the resistive load R = 70 Ω.

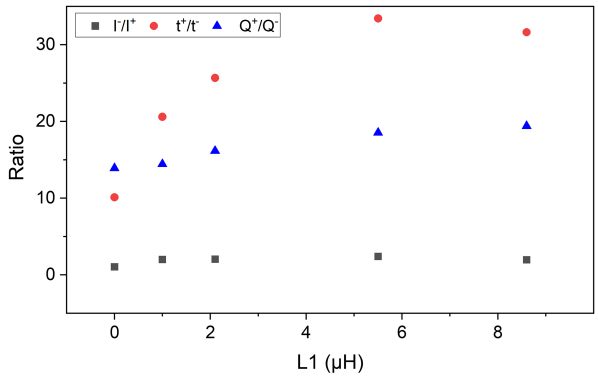

Fig. 10. Ratios of the pumping currents (square), pumping times (round) and electric charges (triangle) as a function of the inductance L1 obtained for the OTS-100 at the resistive load R = 50 Ω and charging voltage V_{C1} = 6 kV.

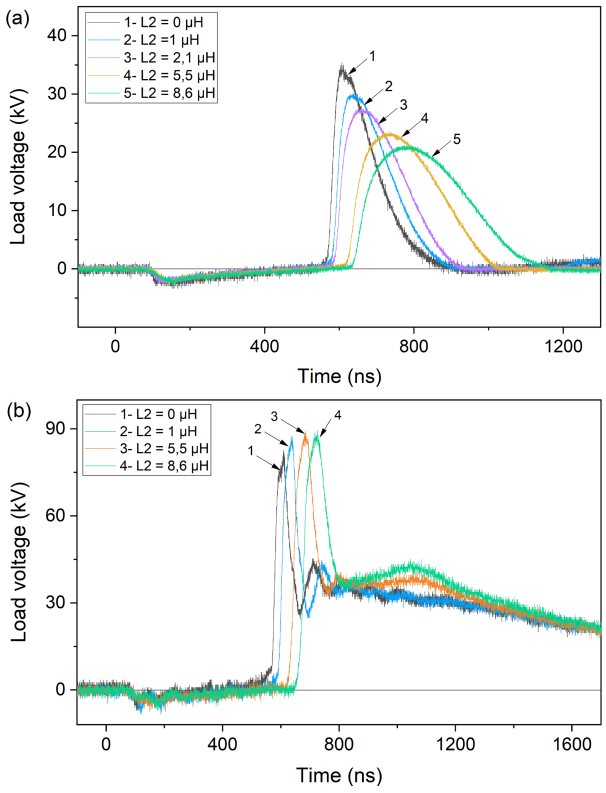

Fig. 11. Load voltage at different L2 on 50 Ω load (a), and on 1 kΩ load (b) using the OTS-100 diode at charging voltage V_{c1} = 6 kV.

1.3 without approaching the SOS-180-4 diode current ratio of 3.2. It is worth mentioning a constant ratio of the forward and reverse electric charges Q^+/Q^- calculated as $Q = \int i(t)dt$ during the diode forward and reverse pumping. For this experiment, the bias current (Ib in Fig. 9(b)) was fixed at zero for V_{C1} from 3 kV to 5 kV; at 1 A for V_{C1} from 6 kV to 7 kV; at 2 A for V_{C1} from 8 kV to 9 kV; and 3 A for V_{C1} = 10 kV.

To examine the impact of the I^- magnitude on the OTS-100 switching, an additional inductance L1 has been added in series with the capacitor C1, shown in Fig. 6. The Fig. 10 summarizes the results. The inductance L1 was varied from 0 to 8.6 μH, causing the variation of I^- from 0.4 kA to 0.1 kA. During these experiments, I^+ and t^+ were changing as well, while t^- remained constant. For this experiment, a 50 Ω TVO less-inductive resistor load is used. The charging voltage V_{C1} was fixed at 6 kV. It was noticed that increasing L1 causes the forward current duration to increase and the forward and reverse current amplitudes to decrease, while the reverse current duration remains about the same. This results in an increasing of the ratio I^-/I^+ to 2.4. The t^+/t^- ratio obviously increases, as well as the forward to reverse electric charges.

High values of the inductance L1 leads to a decrease in the maximum voltage at C2 and, therefore, lower voltage across the load. Although the current ratio I^-/I^+ is improved by adding L1, the load current and voltage amplitudes drop, thus the use of a less inductive primary circuit is recommended.

According to the literature [3], a nanosecond current cutoff in semiconductor diodes with a switching power from MW to GW can be realized using the drift step recovery diode

TABLE II
LOAD VOLTAGE AMPLITUDE, RISE TIME, WIDTH AND ENERGY EFFICIENCY AT DIFFERENT L2 ON 50 Ω AND 1 kΩ ($\eta = \frac{E_R}{E_{C1}}$)

R (Ω)	***L2*** (μH)	V_R (kV)	T_r (ns)	***FWHM*** (ns)	η (%)
50	0	35	23	116	58
	0.3	32	26	130	55
	1.0	30	29	150	56
	5.5	24	53	250	55
	8.6	21	71	290	55
1000	0	83	21	63	44
	0.3	84	24	64	43
	1.0	86	28	65	42
	5.5	88	33	85	46
	8.6	87	34	105	48

(DSRD) or the semiconductor opening switch. However, it seems that the results obtained in this work can not be fully explained by these two mechanisms. While the limit of DSRD is 200-300 A/cm² [3], in the present work the OTS-100 diode operates at a current density of more than 1 kA/cm², which is usually considered as a threshold of the SOS mode [7]. Also, even though the OTS-100 was tested at forward pumping mode required to the SOS mechanism, reverse pumping mode parameters were dramatically different from those expected from an SOS diode.

In particular, reverse pumping time t^-, which was limited by the reverse conductivity of the diode, was two times less compared to the SOS-180-4 diode. What is more important, t^- is almost insensitive to the forward pumping parameters such as t^+ and I^+. However, the cutoff time of the OTS-100 diode (tens of nanoseconds) is close to an SOS diode cutoff time at comparable voltage and power levels on the load. These facts probably require another mechanism of current interruption to be considered. At this moment, it is assumed that specific diode structure - engineered for a fast recovery - could be a reason for the fast current cutoff. However, to shed light on this question, one needs to know the exact doping profile of the diode, which is usually a trade secret of the manufacturer.

Finally, the inductance L2 (Fig. 6) was installed to investigate its impact on the shape of the output voltage and on the energy transferred to the load. An experiment was performed on 50 Ω and 1 kΩ loads with L1 = 0. The results are presented in Fig. 11(a) and Fig. 11(b); and Table II summarizes the parameters of the output voltage pulse and the energy efficiency as a function of the inductance L2. The energy delivered into the load is numerically estimated as the integral of the load power. The stored energy in the capacitor is calculated as the half product of the capacitance and the square of the voltage ($E_{C1} = \frac{C_1 U_{C1}^2}{2}$).

As shown in Fig. 11(a) for the low-impedance load, the inductance L2 reduces the amplitude of the load voltage pulse and increases pulse duration. The rise time is also extended and the input to output energy efficiency is not improved (Table II). On the contrary, for high-impedance loads (Fig. 11(b)), L2 improves, in the first instance, the high-voltage part of the voltage pulse. The amplitude and duration of the high-voltage part are probably increased due to an increase in the energy stored in L2, which changes from 80 mJ to 260 mJ for L2 equal to 1 μH and 8.6 μH, respectively. In addition, the energy efficiency is slightly improved, though the rise time is increased (Table II).

IV. CONCLUSION

The use of off-the-shelf diodes as semiconductor opening switches has been investigated. Among the 25 off-the-shelf diodes tested with the low-energy test bench, the TVS diodes showed the best results in terms of switching time. The switching power of the off-the-shelf diodes was increased by series-parallel connection. Series connection of the off-the-shelf diodes increased the voltage capability of the switch, whereas parallel connection reduced its energy losses. It was shown that the output voltage can be linearly adjustable using a variable primary charging voltage combined with an appropriate resetting current. In order to optimize the energy efficiency of the circuit, the inductance of the primary circuit of the transformer should be minimized, while an appropriate secondary inductance should be determined depending on the load. The off-the-shelf diodes have shown a good stability in voltage switching after a large number of shots, with no degradation of the diodes being observed during experimentation. When combined with a solid-state primary switch and the implementation of an efficient cooling, the off-the-shelf diode assemblies represent a serious candidate to become a major asset in the development of high repetition rate nanosecond pulsed power systems.

REFERENCES

[1] H. Bluhm, *Pulsed Power Systems: principles and applications*. Springer, Berlin, Heidelberg, 2006.

[2] S. N. Rukin, "Pulsed power technology based on semiconductor opening switches: A review," *Review of Scientific Instruments*, vol. 91, 2020.

[3] I. V. Grekhov and G. A. Mesyats, "Nanosecond semiconductor diodes for pulsed power switching," *Physics-Uspekhi*, vol. 48, no. 7, pp. 703–712, 2005.

[4] S. Scharnholz, V. Brommer, G. Buderer, and E. Spahn, "High-power MOSFETs and fast-switching thyristors utilized as opening switches for inductive storage systems," *IEEE Transactions on Magnetics*, vol. 39, no. 1 I, pp. 437–441, 2003.

[5] W. Jiang, K. Yatsui, K. Takayama, M. Akemoto, E. Nakamura, N. Shimizu, A. Tokuchi, S. Rukin, V. Tarasenko, and A. Panchenko, "Compact solid-state switched pulsed power and its applications," *Proceedings of the IEEE*, vol. 92, no. 7, pp. 1180–1195, 2004.

[6] I. V. Grekhov and G. A. Mesyats, "Physical basis for high-power semiconductor nanosecond opening switches," *IEEE Transactions on Plasma Science*, vol. 28, no. 5, pp. 1540–1544, 2000.

[7] G. A. Mesyats, S. N. Rukin, S. K. Lyubutin, S. A. Darznek, Y. A. Litvinov, V. A. Telnov, S. N. Tsyranov, and A. M. Turov, "Semiconductor opening switch research at iep," *Proceedings of the 10th IEEE International Pulsed Power Conference, Albuquerque, New Mexico, USA*, pp. 298–305, 1995.

[8] S. A. Darznek, G. A. Mesyats, S. N. Rukin, and S. N. Tsyranov, "Theoretical model of the sos effect," *Proceedings of the 11th International Conference on High Power Particle Beams, Prague, Czech Republic, June 10–14, 1996*, pp. 1241–1244, 1996.

[9] S. N. Rukin, "High-power nanosecond pulse generators based on semiconductor opening switches (review)," *Instrument and experiment Techniques*, pp. 439–467, 1999.

[10] G. Wang, J. Su, Z. Ding, X. Yuan, and Y. Pan, "A semiconductor opening switch based generator with pulse repetitive frequency of 4 MHz," *Review of Scientific Instruments*, vol. 84, no. 12, pp. 9–12, 2013.

[11] S. K. Lyubutin, M. S. Pedos, A. V. Ponomarev, S. N. Rukin, B. G. Slovikovsky, S. N. Tsyranov, and P. V. Vasiliev, "High efficiency nanosecond generator based on semiconductor opening switch," *IEEE Transactions on Dielectrics and Electrical Insulation*, vol. 18, no. 4, pp. 1221–1227, 2011.
[12] S. Y. Sokovnin and M. E. Balezin, "Improving the operating characteristics of an YPT-0.5 accelerator," *Instruments and Experimental Techniques*, vol. 48, no. 3, pp. 392–396, 2005.
[13] ——, "Repetitive nanosecond electron accelerators type URT-1 for radiation technology," *Radiation Physics and Chemistry*, vol. 144, no. April 2016, pp. 265–270, 2018.
[14] T. Tang, F. Wang, A. Kuthi, and M. A. Gundersen, "Diode opening switch based nanosecond high voltage pulse generators for biological and medical applications," *IEEE Transactions on Dielectrics and Electrical Insulation*, vol. 14, no. 4, pp. 878–883, 2007.
[15] T. Sugai, W. Liu, A. Tokuchi, W. Jiang, and Y. Minamitani, "Influence of a circuit parameter for plasma water treatment by an inductive energy storage circuit using semiconductor opening switch," *IEEE Transactions on Plasma Science*, vol. 41, no. 4, pp. 967–974, 2013.
[16] T. Sugai, W. Jiang, and A. Tokuchi, "Influence of forward pumping current on current interruption by semiconductor opening switch," *IEEE Transactions on Dielectrics and Electrical Insulation*, vol. 22, no. 4, pp. 1971–1975, 2015.
[17] A. S. Kesar, A. Raizman, G. Atar, S. Zoran, S. Gleizer, Y. Krasik, and D. Cohen-Elias, "A fast avalanche Si diode with a 517 μ m low-doped region," *Applied Physics Letters*, vol. 117, no. 1, 2020.
[18] K. Takaki, I. Yagi, S. Mukaigawa, T. Fujiwara, and T. Go, "Ozone synthesis using streamer discharge produced by nanoseconds pulse voltage under atmospheric pressure," *PPC2009 - 17th IEEE International Pulsed Power Conference*, no. December 2015, pp. 989–993, 2009.
[19] A. I. Gusev, S. K. Lyubutin, A. V. Ponomarev, S. N. Rukin, and B. G. Slovikovsky, "Semiconductor opening switch generator with a primary thyristor switch triggered in impact-ionization wave mode," *Review of Scientific Instruments*, vol. 89, no. 11, p. 114702, nov 2018.
[20] Vacuumschmelze. Nanocrystalline material. [Online]. Available: https://www.vacuumschmelze.com/Nanocrystalline-Material
[21] J. Choi, "Introduction of the magnetic pulse compressor (MPC) - Fundamental review and practical application," *Journal of Electrical Engineering and Technology*, vol. 5, no. 3, pp. 484–492, 2010.
[22] A. V. Ponomarev, S. N. Rukin, and S. N. Tsyranov, "Investigation of the process of voltage distribution over elements of a high-power semiconductor current interrupter," *Technical Physics Letters*, vol. 27, no. 10, pp. 857–859, 2001.
[23] J. Holma and M. J. Barnes, "Prototype Inductive Adders with Extremely Flat-Top Output Pulses for the Compact Linear Collider at CERN," *IEEE Transactions on Plasma Science*, vol. 46, no. 10, pp. 3348–3358, 2018.

Mawuena R. Degnon (Student member, IEEE) was born in Lomé, Togo in 1996. He received his M.Sc. in electrical engineering and industrial computing from the Université de Pau et des Pays de l'Adour (UPPA), Pau, France in 2020 after his M.Eng. in electrical engineering received from the Université de Lomé, Lomé, Togo in 2018. He is currently pursuing the Ph.D. degree with the department of electrical engineering of the UPPA. His research interests include high-voltage pulsed power systems, solid-state switches and nanosecond high-voltage generators for industrial applications.

Anton I. Gusev (Member, IEEE) was born in Miass, Russia, in 1988. He received his M.S. degree in electrophysics (2012) from the Ural Federal University (UrFU) and his Ph.D. degree in engineering sciences (2019) from the Institute of Electrophysics of the Ural Branch of the Russian Academy of Sciences (IEP) in Yekaterinburg, Russia. From 2008 to 2019, he has been with IEP as an Intern, Ph.D. Student, and Junior Researcher in the Pulsed Power Laboratory. At the same time, from 2014 to 2019, he has been with UrFU as a Senior Teacher. In 2019, he became a Postdoc at the Université de Pau et des Pays de l'Adour (UPPA) in Pau, France. Since 2020, he is an Assistant Professor in the SIAME laboratory at UPPA. His research interests include semiconductor physics, high-power semiconductor switches, and high-voltage solid-state generators, which provide nano- and subnanosecond pulses. Dr. Gusev is a member of the International Society on Pulsed Power Applications (ISP) and the Association for the Advancement of Pulsed Power (A2P2). He has been awarded as a young researcher at major international pulsed power conferences (EFRE 2016, EAPPC 2018, GDP 2021) including two supported by IEEE (PPC 2017 and IPMHVC 2018).

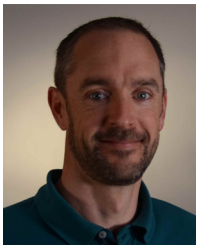

Antoine Silvestre de Ferron was born in Tarbes, France, in 1977. He received the master degree in electrical and electronic engineering from the University of Toulouse, Toulouse, France, and the Ph.D. degree in electrical engineering from the University of Pau, Pau, France, in 2002 and 2006, respectively. From 2006 to 2008, he was a Researcher with the Atomic Energy Commission (CEA), a French government-fund technological research organization in Le Barp, France. He is currently an engineer at the head of the High Voltage Processes Teams in the SIAME laboratory of the University of Pau, France. His research interests include high-pulsed power generation, with military and civil applications. He is specialized in Marx generator and pulse forming lines in high voltage generation, in high voltage transient probes associated and in high current discharges in liquids.

Laurent Pecastaing (M'13-SM'17) he received the Ph.D. and Research Directorship Habilitation degrees in electrical engineering from the Université de Pau et des Pays de l'Adour (UPPA), Pau, France, in 2001 and 2010, respectively. He is currently a Full Professor in pulsed power with University of Pau. He is the director of the SIAME laboratory, and he is also the Director of a Common Laboratory between UPPA and CEA, France. His current research interests include high-power microwave sources, compact pulsed power systems, and ultrafast transient probes. Dr. Pécastaing was the Chairman of the EAPPC/BEAMS/MEGAGAUSS Conference in France in 2021. He is also a member of the International Steering Committees for both the BEAMS Conferences and the Euro-Asian Pulsed Power Conferences.

Gaëtan Daulhac was born in Brive la Gaillarde, France, in 1987. He graduated from the ENSIAME and he received a research master degree from the Université de Valencienne (UVHC), Valenciennes, France in 2010. He is currently an Engineer at ITHPP. He works on high pulsed power generator. More precisely, on resonant generator, dedicated to pulse electron beams sterilization.

Aleksandr Baranov received his Master of Engineering (M.Eng.) in Industrial Electrical Energy and Engineering from Togliatty State University, Togliatty, Russia, in 2015. He is currently R&D engineer in ITHPP, Thégra, France. His research fields of interests are high-voltage nanoseconds generators, electron emission and pulsed power systems.

Sebastien Boisne Sébastien BOISNE was born in Thionville, France, in 1979. He holds a Master's degree in Global Management of Organizations, Strategy and Finance from the University of Paris Dauphine PSL. In 2002, he joined Thomson CSF Linac, Orsay, France, a leader in linear electron accelerators, where he is in charge of the development of electron beam range of products, intended to be employed in high demands industrial uses. He is currently at the head of BETA BEAMS (ITHPP-ALCEN group), Donzenac, France, specializing in the design and supply of electron beam accelerators, installed on end-users production sites, and mainly used in surface and core sterilization of pharmaceutical products.

Bucur M. Novac (Senior Member, IEEE) received the M.Sc. and Ph.D. degrees from the University of Bucharest, Bucharest, Romania, in 1977 and 1989, respectively. He joined Loughborough University, Loughborough, U.K., in 1998, where he is currently a Professor of pulsed power. His research interests include compact and repetitive high-power systems, explosively and electromagnetically driven magnetic flux compression generators and their applications, electromagnetic launchers, ultrafast magneto and electro-optic sensors, and 2-D modeling of pulsed power systems. He has coauthored two books on explosive pulsed power and has published more than 200 refereed articles and conference contributions. Prof. Novac is a member of the International Steering Committees for the MEGAGAUSS Conference and the Euro-Asian Pulsed Power Conference (EAPPC). He is a fellow of the Royal Academy of Engineering and a Chartered Engineer and a fellow of the Institution of Engineering and Technology, U.K. He was a Voting Member of the Pulsed Power Science and Technology Committee of the IEEE Nuclear and Plasma Science Society, a member of the Organizing Committee of the IEEE International Power Modulator and High Voltage Conference, and the Co-Chairman of the U.K. Pulsed Power Symposia.